Testing of Alternative Spiral Bevel and Hypoid Gear Theory

W. R. Winfough and D. B. Dooner

Following is a presentation of a gear design based upon a theoretically perfect gear technology, for which an overview is offered for consideration. What follows is a report on the design's testing and subsequent manufacture of a hypoid gear pair for a 1999 Ford Mustang.

Background

A system of curvilinear coordinates is presented to describe general bevel and hypoid gear elements. Subsequently this system of coordinates is used for the mathematical development of fundamental relations describing general gear pairs. One set of relations is defined as the *Three Laws of Gearing*. An overview of these three laws is presented to help demonstrate the capabilities of this theoretically perfect theory for spiral bevel and hypoid gear design vs. existing practice for the design and manufacture of spiral bevel and hypoid gear elements. This gear theory can be used to produce any gear form shape.

Cylindroidal Coordinates

A system of curvilinear coordinates (u, v, w) is introduced to describe spiral bevel and hypoid gears. The coordinates (u, v, w) used to parameterize these families of pitch, transverse, and axial surfaces are formulated using the cylindroid defined by the input and output axes of rotation. A design methodology for spatial gearing analogous to cylindrical gearing begins with the equivalence of friction cylinders (Fig. 1). These generalized friction surfaces are two ruled surfaces determined by the instantaneous generator. The transmission of motion between the two generally disposed axes, $\$_i$ and $\$_o$, via two friction surfaces requires knowledge of the instantaneous generator. The location of the instantaneous generator relative to the two axes $\$_i$ and
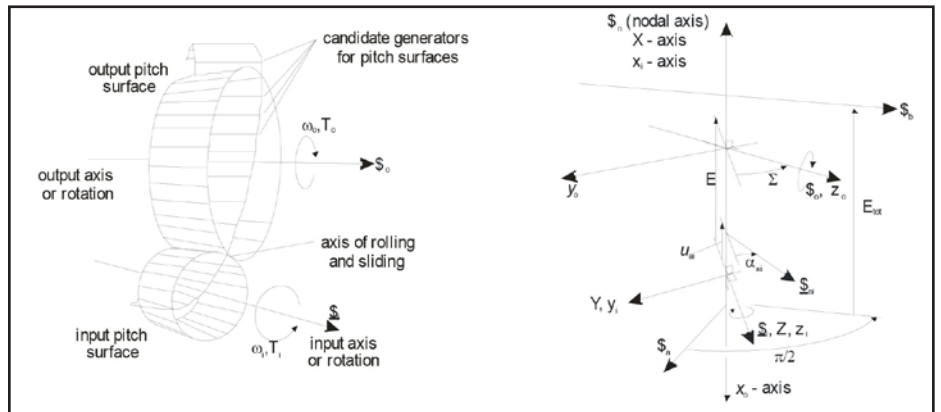

Figure 1   Two hyperboloidal friction wheels for motion transmission between skew axes.

$\$_o$ depends upon the distance E along the common perpendicular to rotation axes $\$_i$ and $\$_o$, the angle D between axes of rotation $\$_i$ and $\$_o$, and the magnitude of the gear ratio g.

The synthesis of a spatial three-link gear mechanism is similar to the synthesis of the planar three-link geared mechanism. The twist displacement of one Body relative to another Body is denoted by $dv\$$, where dv is the magnitude of the twist $\$$. The relationship for the twist displacements of three bodies is:

$$dv_{12}\$_{12} + dv_{23}\$_{23} + dv_{31}\$_{31} = 0 \tag{1}$$

where:
$dv_{12}\$_{12}$ is the relative displacement of Body 2 with respect to Body 1
$dv_{23}\$_{23}$ is the relative displacement of Body 3 with respect to Body 2
$dv_{31}\$_{31}$ is the relative displacement of Body 1 with respect to Body 3

Body 1 represents ground; Body 2 is the input Body; and Body 3 is the output Body. If $dv_i\$_i$ is the twist displacement (pure rotation) of the input with respect to ground, $dv_{is}\$_{is}$ is the twist displacement of the output Body relative to the input Body, and $dv_o\$_o$ is the twist displacement of the output Body relative to ground, then the vector loop (Eq. 1) for the spatial three-link mechanism becomes:

$$dv_i\$_i + dv_{is}\$_{is} - dv_o\$_o = 0 \tag{2.a}$$

Dividing by dt, its significance to gearing is:

$$\omega_i\$_i + \omega_{is}\$_{is} - \omega_o\$_o = 0 \tag{2.b}$$

where:
ω_i angular speed of input gear
ω_{is} angular speed of output gear relative to input gear
ω_o angular speed of output gear
$\$_i$ zero-pitch twist coordinates of input axis of rotation
$\$_{is}$ homogeneous twist coordinates of IS (instantaneous screw)
$\$_o$ zero-pitch twist coordinates of output axis of rotation

The *transmission function* is the functional relationship between the angular position v_i of an input element and the corresponding angular position v_o of a mating output gear element. The instantaneous gear ratio g is the ratio between the instantaneous, angular displacement dv_o of the output and the corresponding, instantaneous angular displacement dv_i of the input, thus:

$$
g \equiv \frac{dv_0}{dv_1} = \frac{\text{infinitesimal angular displacement of the output body}}{\text{infinitesimal angular displacement of the input body}} \tag{3}
$$

The displacements dv_i and dv_o are about the input and output axes $\$_i$ and $\$_o$, respectively. The angular speeds ω_i and ω_o are, respectively, the angular displacements dv_i and dv_o per-unit time d_t. The kinematic geometry of toothed bodies is independent of time t and, hence, speed ω_i of the input. Rearranging Equation 2b, $dv_{is}\$_{is}$ becomes:

$$
dv_{is}\$_{is} = -dv_i(\$_i - g\$_o) \tag{4}
$$

Axodes are ruled surfaces that roll and slide upon one another in a special way. In order to distinguish which pitch surface is the axode, the "theorem of three axes" will be applied to the two special twists $\$_i$ and $\$_o$. A fixed reference frame (X, Y, Z), an input reference frame (x_i, i_y, z_i), and an output reference frame (x_o, y_o, z_o) are used to parameterize these pitch surfaces. The screw axis $\$_i$ of the input reference frame coincides with the Z axis of the fixed reference frame. The distance E—along the common perpendicular between the input and output axes $\$_i$ and $\$_o$—is along the positive X axis of the fixed reference frame. The z_o axis of the output reference frame is perpendicular to the X axis of the fixed reference frame.

Two systems of curvilinear coordinates based on the cylindroid are used to parameterize toothed bodies in mesh. An input Cartesian coordinate system (x_i, y_i, z_i) is introduced where the z_i axis is aligned with the input's axis of rotation and the x_i axis is along the common perpendicular. An output Cartesian coordinate system (x_o, y_o, z_o) is introduced where the z_o axis is aligned with the output's axis of rotation, and the x_o axis is along the common perpendicular. Twist coordinates $\$_i$ used to parameterize the displace-

ment of the input body are shown in Figure 1 where:

$$
\$_i = (0, 0, 1; 0, 0, 0),
$$

and the twist coordinates $\$_o$ used to define the displacement of the output body are:

$$
\$_o = (0, -\sin\Sigma, \cos\Sigma; 0, -E\cos\Sigma, -E\sin\Sigma).
$$

Applying the theorem of three axes given by Equation 4, the twist coordinates $dv_{is}\$_{is}$ are used to determine the relative displacement between the input body; the output body then become $dv_{is}\$_{is} = dv_i(0, -g\sin\Sigma, g\cos\Sigma - 1; 0, -gE\cos\Sigma, -gE\sin\Sigma).$

The intersection between the ISA and the fixed X axis can be expressed as:

$$
r \times C_{is} = Ç_{is} - h_{is}C_{is} \tag{5}
$$

where:
r is the point of intersection between the fixed X axis and the twist $dv_{is}\$_{is}$
h_{is} is the pitch of the twist $dv_{is}\$_{is}$
and:
$(C_{is}, Ç_{is})$ are the twist coordinates of $dv_{is}\$_{is}$
Crossing C_{is} into the above relation and expanding

$$
r = \frac{C_{is} \times Ç_{is}}{C_{is} \cdot C_{is}} \tag{6}
$$

since $r \perp C_{is}$.

Substituting values for C_{is} and $Ç_{is}$ into Equation 6, $r = u_{ai}i_i$, where the radius u_{ai} of the input axode is:

$$
u_{ai} = E_g \frac{g - \cos\Sigma}{1 + g^2 - 2g\cos\Sigma} \tag{7}
$$

The Plücker coordinates of the generators for the input axode are specified in terms of the direction cosines C_{ai} for an arbitrary angular position v_i of the input. The included angle α_{ai} between the instantaneous screw axis and the input axis $\$_i$ is defined as the cone angle. Projecting the free vector C_{is} onto the input axis $\$_i$, the cone angle α_{ai} becomes:

$$
\alpha_{ai} = \tan^{-1}\frac{-g\cos\Sigma}{1 - g\cos\Sigma} \tag{8}
$$

The axode is *left-handed* when the cone angle α_{ai} is positive about the x_i axis. A positive displacement dv_i of the input gear must be accompanied with a negative parameterization of the axode. Thus the free vector part C_{ai} for the generators of the input axode becomes:

$$
C_{ai} = (-\sin\alpha_{ai}\sin v_i)i_i + (-\sin\alpha_{ai}\cos v_i)j_i + (\cos\alpha_{ai})k_i \tag{9a}
$$

If r_{ni} denotes the coordinates of the neck, then the moment part $Ç_{ai}$ is expressed as:

$$
Ç_{ai} = r_{ni} \times C_{ai} \tag{9b}
$$
$$
\text{where } r_{ni} = u_{ai}(\cos v_i i_i - \sin v_j j_i).
$$

The Plücker coordinates for the generators of the output axode are similar to those of the input axode.

A *transverse surface* is an infinitesimally thin surface used to parameterize conjugate surfaces for direct contact between two axes. Each angular position v_i and axial position w_i define a unique point p in space for a given g. The point p traces a curve in space as g varies from $-\infty$ to ∞. Another value of the input position v_i defines the same cylindroid. It is this two-parameter loci of points p that compose the transverse surface. The Cartesian coordinates r for the single point p on the generator $\$_{ai}$ are:

$$
r = u_i i_i - w_i \sin\alpha_i j_i + w_i \cos\alpha_i k_i \tag{13}
$$

Rotating the above curve r about the z_i axis, an amount v_i leads to:

$$
r = \begin{bmatrix} \cos v_i & \sin v_i & 0 \\ -\sin v_i & \cos v_i & 0 \\ 0 & 0 & 1 \end{bmatrix} \begin{bmatrix} u_i \\ -w_i\sin\alpha_i \\ w_i\cos\alpha_i \end{bmatrix} \tag{14}
$$

The *axial surface* provides the relationship between successive transverse surfaces. For each value of v_i, the axial surface is the locus of generators determined by g, where $-\infty < g < \infty$. The
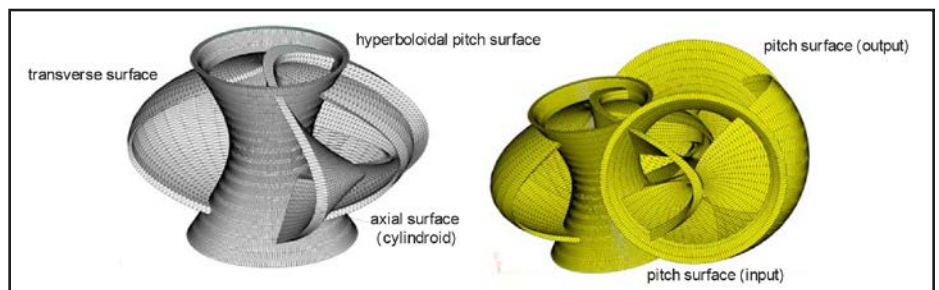

Figure 2 Pitch, transverse, and axial surface for uniform motion transmission.

curves defined by holding two of the three parameters — u, v, and w constant — are coordinate curves. Two parameters used to define a surface are the curvilinear coordinates of that surface; i.e. — the pitch surface by v_i and w_i (u_i = constant); the transverse surface by u_i and v_i (w_i = constant); and the axial surface by ui and wi (v_i = constant). Shown in Figure 2 are a set of pitch, transverse, and axial surfaces using cylindroidal coordinates (u_i, v_i, w_i).

The Three Laws of Gearing

Three laws of gearing are presented in terms of toothed bodies in mesh or gear pairs. Present day design and manufacturing techniques make approximations to the ideal conditions necessary for motion transmission — resulting in limitations in face width, number of teeth in mesh, spiral angle, and pressure angle. The three laws of gearing are established in terms of a three-link, 1-dof mechanism.

Three laws of gearing:

1. Defines the relation between the tooth surface normal and the desired gear ratio
2. Establishes the relation between pitch surfaces, spiral angle, and desired gear ratio for any tooth profile
3. Establishes the relative curvature between tooth surfaces in direct contact.

Gear pairs are special, direct-contact mechanisms where motion is achieved by surfaces in direct contact. Depicted in Figure 3 are the input axis of rotation $\$_i$, the output axis of rotation $\$_o$, and the instantaneous screw axis $\$_{isa}$ along with the tooth contact normal $\$_l$. Shown is the shaft center distance E between the two axes of rotation $\$_i$ and $\$_o$, along with the included angle Σ between these two axes. Invoking Ball's reciprocity condition between the line of action $\$_l$ and the vector loop Equation 2a yields:

$$\$_l \bullet (dv_i\$_i + dv_{is}\$_{is} - dv_o\$_o) = 0 \qquad (15)$$

Specifying that the reciprocal product between the line of action $\$_l$ and the instantaneous twist $\$_{is}$ is zero (i.e., $dv_{is}\$_{is}\$_l$), the above relationship is rearranged to:

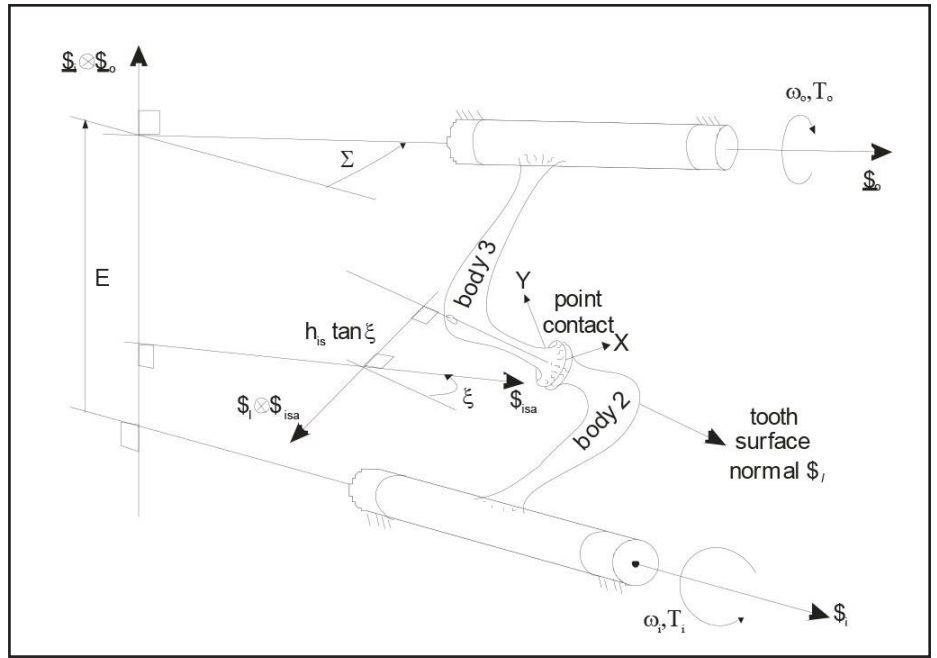$$g = \frac{\$_l \circ \$_i}{\$_l \circ \$_o} \qquad (16)$$

Figure 3   Relation between input axis $\$_i$, output axis $\$_o$, ISA $\$_{isa}$, and contact normal $\$_l$.

where:
  g instantaneous gear ratio
  $\$_l$ homogeneous screw coordinates of tooth contact normal
  $\$_i$ homogeneous twist coordinates of input axis of rotation
  $\$_o$ homogeneous twist coordinates of output axis of rotation

Gear tooth mesh — where the tooth surface normal $\$_l$ is reciprocal to the desired twist $\$_{is}$ — is defined as conjugate action. The above relation is independent of the contact position between the two gear elements and depends only on the line of action $\$_l$ and axes $\$i$ and $\$_o$. The first law of gearing can be stated as:

For motion transmission between two axes via two gear teeth in direct contact, the contact normal to the two gear teeth in direct contact must be reciprocal to the instantaneous twist defined by the two axes of rotation, and the gear ratio in order to achieve the desired instantaneous gear ratio.

The cited first law of gearing is a generalization of Euler's original "Laws of Gearing." It encompasses noncircular gears where the position of the pitch point varies in addition to spatial gearing, where the common tooth normal does not intersect the generator of the axodes or the instantaneous screw axis.

The orientation of the gear tooth on the pitch surface must ensure that the desired gear ratio is maintained. The orientation is based on two angles — a

pressure and spiral angle. The independence of pressure angle from spiral angle is explained in terms of the linear line complex defined by the twist $\$_{is}$ (Ref. 1). Such specification of spiral angles de-couples the spiral angle from the pressure angle, and the second law of gearing can be stated as:

For motion transmission between two axes via two gear teeth in direct contact: in order to achieve the desired instantaneous gear ratio for any pressure angle, the spiral angle on the reference pitch surface must be determined by the planar pencil of contact normals reciprocal to the instantaneous twist defined by the two axes of rotation and the gear ratio.

Gear tooth geometry at a point on the pitch surface can be specified in terms of the normal curvature and geodesic torsion of two separate curves on the tooth surface. These separate curves are the line of contact and the intersection between the gear tooth and the reference pitch surface (the tooth spiral). Knowledge of the curvature and torsion between these two curves embedded in the gear tooth surface uniquely define the gear tooth curvature; this relation is independent of the tooth type. Together these expressions are used to establish a fundamental relation for the relative curvature of two conjugate surfaces in direct contact; thus the third law of gearing can be stated accordingly:

For uniform motion transmission between two axes via two teeth in direct contact, relative curvature between the two teeth in direct contact depends on the gear ratio, the spiral angle and pressure angle, and is independent of the gear tooth geometry.

Comparison to Old Technology

An overview of face cutting methods for spatial gear design and manufacture is provided by Shtipelman (Ref. 1), Stadtfeld (Refs. 2-3) and Litvin-Fuentes (Ref. 4). Below are three companies providing machines and machine tools used to produce crossed-axes gear pairs:

- The Gleason Works (*www.gleason.com*)
- Klingelnberg-Oerlikon (*www.klingelnberg.com*)
- Yutaka Seimitsu Kogyo, Ltd.*(www.yutaka.co.jp).*

Figure 4 displays circular face cutters used today for fabricating spiral bevel and hypoid gear elements. The ideal shape of hyperboloidal gears cannot be produced using circular face cutters, resulting in restrictions on candidate gear designs. One goal of the presented approach is to establish a new method for the fabrication of hyperboloidal gears that overcomes certain limitations of existing face cutting technology.

Design, Manufacture, Testing

Over 75% of manufactured spiral bevel and hypoid gears are utilized in automotive and locomotion activities. This test showcases the benefits of the perfect transmission computational method. The intent is to demonstrate that *theoretically* perfect gears, which, ultimately, will be manufactured using a hob for hypoid, spiral bevel and skew axis gearing, is in fact robust and as functional as the current face hobbing process for spiral bevel and hypoid gears. A 1999 Ford Mustang coupe was chosen as the test vehicle. The Ford Mustang came with a Ford 7.5-inch, 2.93 ratio hypoid rear end, and a V6 small block.

The availability of the details associated with all engineered products, like automobiles, is typically considered proprietary to the OEM. Since the OEM specifications for the hypoid gearset were not available, measurements were
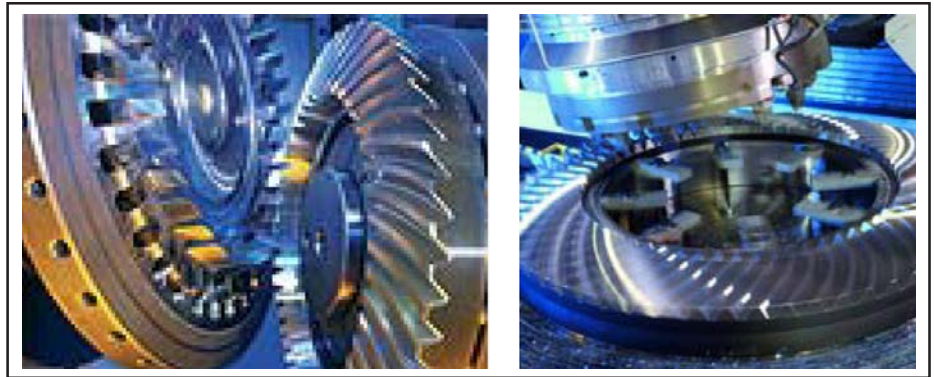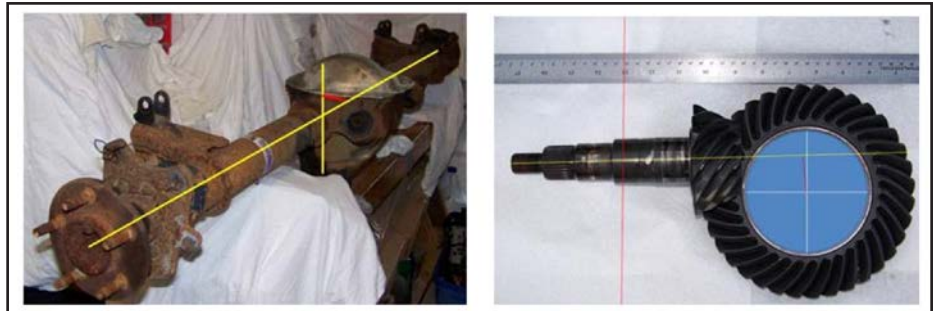

Figure 4   Circular face cutting.

Figure 5   Differential assembly and removed ring and pinion.
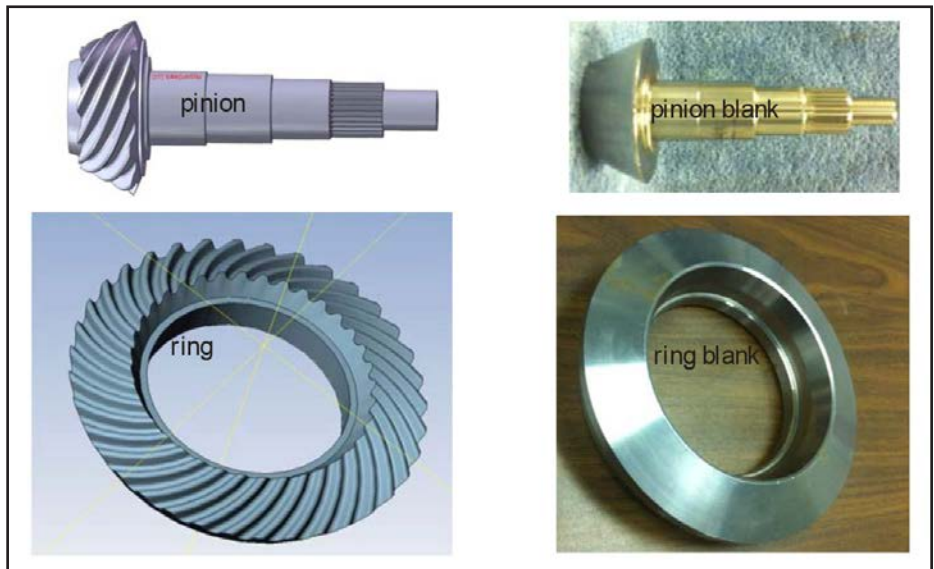

Figure 6   CAD models of pinion and ring gear, along with blanks prior to gear teeth addition.

taken of existing components to complete the design. A replacement rear axle assembly was purchased from a local repair company. The differential case was disassembled and the mounting features were measured and toleranced. Figure 5 shows both the rear axle and the gear pair removed from the assembly.

After extraction of the ring and pinion, a drop-in replacement was designed specific to the application. (The intent of the drop-in replacement was to match the transmission ratio and footprint, given the manufacturing

For Related Articles Search

gear design

at **www.powertransmission.com**

flaws and inability of the original design relative to our theoretically perfect design — essentially creating a direct comparison between the OEM gear pair and the theoretically perfect gear pair.)

Utilizing the mounting features from the OEM parts for mounting dimensions for both the gearbox (differential case) and the gears (ring and pinion), a 3-D model for each of the components was created for proper assembly. Figure 6 shows the 3-D solid model for each of the components.

After completion of the solid model, manufacturing blueprints were created, including standard gearing nomenclature for the precision of each feature. Three sets of gear blanks were started, assuming that we may make a manufacturing or design error (Fig. 6).

The next step in the manufacturing process was to add the teeth. This was done using standard contour milling available with any 5-axis milling machine. Photos of the components prior to heat treatment can be seen in Figure 7.

The next steps in the manufacturing process were to heat treat the components, finish grind the seating features and chase the threads. Final quality control included inspection and pattern check prior to assembly in the test bed. Figure 8 shows the gears set mounted in a gear alignment machine to check the contact pattern. As can be seen, with known perpendicular axes with the proper pinion offset, the pattern runs along the tooth. This is due to the theoretically optimized torque transmission around both axes. The current industry standard cannot achieve this contact pattern using circular face cutters (i.e., both the heel and toe cannot be engaged simultaneously without load-

Figure 7   Ring and pinion prior to heat treatment, along with gears prior to installation.

ing). These methods of manufacturing and computation are patented (Ref.6).

As the pattern was nearly perfect, no lapping was required and the first gearset was sent to shop for installation in our 1999 Ford Mustang. Prior to final assembly a black oxide coating was added to the gears to highlight wear on the tooth flanks during the testing stages (Fig. 7). As these were standard components, a certified Ford mechanic installed the gears.

Figure 9 shows the differential case just before closing after the gear pair had been set up during pattern checking. Both pinion and ring carrier assemblies were adjusted using standard spacers. As can be seen after assembly, the pattern continues to run exactly parallel to the spiral. The pattern is slightly short of the toe as we missed the location of the pinion by about 0.05 mm. But not bad at all for the first one — made and installed for the first time. At this point, the assembly was complete and ready for testing.

Testing for this assembly was conducted prior to disassembly and after replacement for general comparison. Four phases of testing were conducted. The test bed has been driven for over 7,000 miles/11,250 km, while maintaining an overall tested fuel efficiency

of over 30 miles-per-gallon (mpg). The EPA rating for this vehicle was 27 mpg. Figure 10 shows the results of one set of testing. Four sets of testing that each lasted 18 days and about 1,330 miles each. The test route was elevation-neutral and the same fueling location was used at the beginning and end of the route. The route was selected to allow for normal "highway" driving for 74 miles per day. On open stretches, the cruise control speed was recorded and the average speed was calculated by taking the distance recorded on the odometer and dividing by the time collected on a stop watch. The average daily fuel efficiency is also plotted. All four phases averaged over 30 mpg. This is a fuel efficiency of more than 10% better than the "highway mileage" published at *epa.gov* for this vehicle.

The four lines shown in Figure 10 are the distance traveled each day — nearly a flat line at 74 miles. The blue line shows the "cruise control" speed used on the open stretches — about 80% of the trip. The red line is the average speed calculated using the odometer reading and a stopwatch. Lastly, the fuel economy was recorded daily. This was done using the same gas pump at the same gas station and recording the daily fuel added to the tank divided into
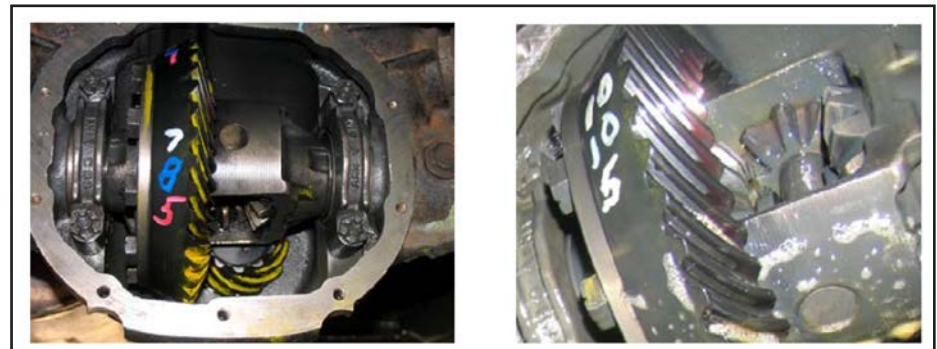

Figure 8   Pattern check after heat treatment and grinding to test seating features.

Figure 9   Ring and pinion installed with shim settings marked; wear check 8,200 km.

the distance traveled. Some fluctuation is expected for fuel economy and average speed, as this was a road course with the normal, other influences including rain, traffic, wind and other variations in driving conditions.

The last telling point was to look at the wear of the ring and pinion in application. Figure 9 shows the freshly washed gears after Phase 3 of the testing and 5,100 miles of use. As seen in the gear pair, the wear pattern is easily observed due to the special coating applied. It is clear the wear is absolutely parallel to the tooth. Of note is the extra use of the face width towards the heel of the gear. This implies that with access to the exact design details of the gear box, the same power gears with this design will be able to fully utilize the entire face width. As is commonly known, face width is proportional to power density.

The design, manufacture and testing of these theoretically perfect gears show that this is a viable competitor to other current, empirical solutions available on the market. The gear design cycle for drop-in replacement is two hours; the solid model preparation is 8 hours; and programming the CNC machine is about 40 hours. Effectively — with proper machine availability — from prototype sequence to the beginning of cutting metal can be completed in one work week.

The assembly here was the first set of parts produced for this application and has clearly demonstrated strong performance. The totals for testing to date are over 7,000 miles, with an average fuel economy of 32.0 mpg, 72 days of tests, running 74 miles-per-day. Additional miles occurred as the car was driven without the mileage checks. This is not intended to imply that better than average fuel economy is always possible, but looking at these results, i.e. — no reduction in fuel economy, extremely quiet, no change in wear, extremely fast design cycle — and the fact that these gears are ready for manufacturing in a few days vs. (the current standard) months — this is a viable competitor to the current market offerings. Additionally, it seems logical that optimization of fuel economy from theoretical first principles is likely to come in the future from this design methodology.

In Summary

Demonstrated here is the absolute first gear pair constructed with new technology and methodology, in direct "competition" to currently available market solutions. In aerospace jargon, this new gear pair would be considered the same as "flying the first article." The perfect design methods and reverse engineering resulted pragmatically — fully validating the use of the presented gear technology as a future, preferred gear design methodology. **PTE**

Acknowledgment. D.P. Technologies for the Esprit *license.*

References

1. Dooner, D.B. *Kinematic Geometry of Gearing*, John Wiley & Sons Inc., London, 2012.
2. Delgear (*www.delgear.com*).
3. Shtipelman, B.A. *Design and Manufacture of Hypoid Gears*, John Wiley and Co., New York, 1978.
4. Stadtfeld, H.J. *Manufacturing: Inspection and Optimization — Collected Papers,* The Gleason Works, Rochester, 1995.
5. Litvin, F.L., and A. Fuentes. *Gear Geometry and Applied Theory*, 2nd Ed., Cambridge University Press, London, 2004.
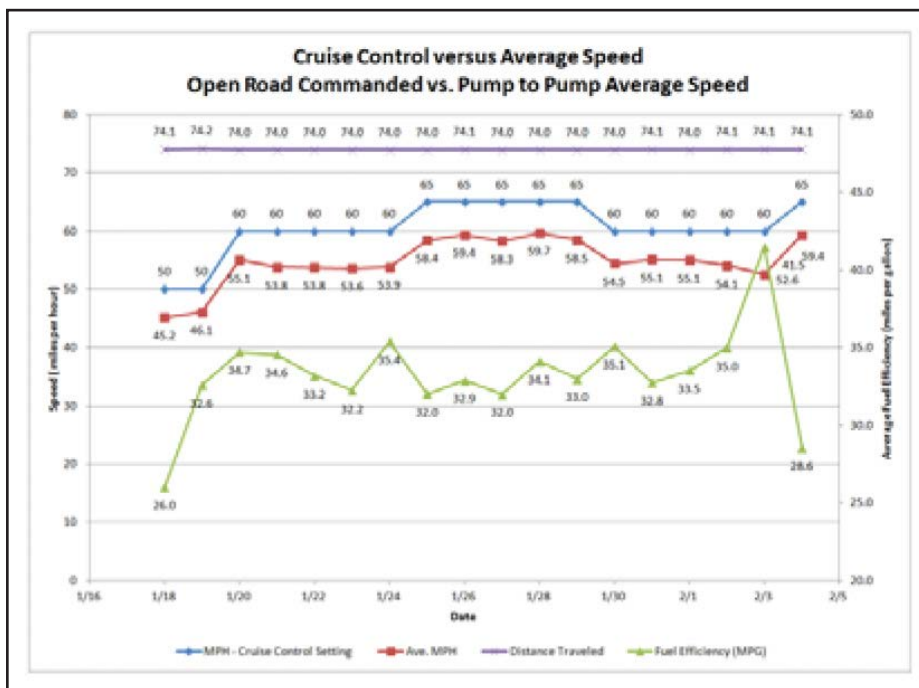6. U.S. Patent 6,449,846: *Gear Manufacturing Method*, Washington, DC, 2002.

Figure 10   Phase I at 18 days, 1,330 miles.

David Dooner graduated from the University of Florida in 1991. Afterwards, he was a visiting scientist with the Russian Academy of Sciences in Moscow and joined the University of Puerto Rico-Mayaguez (UPRM) in 1994. Since joining UPRM, he has been involved with teaching, services, and research. His research focus involves a mathematical approach for the design and manufacture of general hypoid gear pairs. He currently teaches mechanism design, machine design, and senior capstone design. He is currently a member of ASME, ASEE, and AGMA.

Bob Winfough has spent his 20 year career working in various engineering, manufacturing and management roles. He has devoted half of that time to designing and building machining systems, including gear hobbers, shapers and inspection machines. In addition, Winfough spent five years as machining system end user. Over half of his career was on the equity ownership side of the companies for which he worked. Winfough is a member of SME, ASME, Pi Tau Sigma and Tau Beta Pi. He has three earned engineering degrees.